Enhanced Diffraction from a Grating on the Surface of a Negative-Index Metamaterial

D. R. Smith, P. M. Rye, J. J. Mock, D. C. Vier, and A. F. Starr
Department of Physics, University of California, San Diego, La Jolla, California 92093, USA
(Received 19 February 2004; published 23 September 2004)

We show by numerical simulation as well as by measurements on negative-index metamaterial wedge samples, that the unavoidable stepping of the refraction interface—due to the finite unit-cell size inherent to metamaterials—can give rise to a well-defined *diffracted beam* in addition to the negatively *refracted* beam. The direction of the diffracted beam is consistent with elementary diffraction theory; however, the coupling to this higher order beam is much larger than would be the case for a positive index material. The results confirm recent theoretical predictions of enhanced diffraction for negative-index grating surfaces.

DOI: 10.1103/PhysRevLett.93.137405 PACS numbers: 78.20.Ci, 41.20.Jb, 42.25.Fx

Recent demonstrations of artificial materials with negative refractive index (n) have initiated an exploration into the use of these materials to investigate new physics and to develop new applications [1–4]. So many exotic and remarkable electromagnetic phenomena have been predicted to occur in negative-index materials, such as reversed Cerenkov radiation and reversed Doppler shifts [5], that even the most basic of electromagnetic and optical phenomena must be carefully reexamined in the context of negative-index media. For example, in an analysis of the imaging properties of a planar slab of $n = -1$, it has been predicted that resolution exceeding that of any positive index optical component may be realizable [6].

In 2001, an artificial medium composed of two interspersed lattices of conducting elements was fabricated and reported to have a negative-index of refraction [1]. A wedge sample composed of this material, as shown in Fig. 1(a), was demonstrated by Shelby *et al.* [2] to refract microwaves in a manner consistent with the material having a negative refractive index. The medium was composed of a two dimensional arrangement of conducting split ring resonators (SRRs) that provided the equivalent of a negative permeability over a band of frequencies from ~11.0 GHz to 11.5 GHz, and wire strips that provided a frequency band of negative permittivity over a larger and overlapping frequency range.

In the sample used by Shelby *et al.*, the unit-cell size of 5 mm was roughly a factor of 6 smaller than the free space wavelength, so that the material could be expected to be reasonably characterized by effective medium theory. The finite unit-cell size, however, led to an unavoidable stepping of the surface: to achieve the 18.4° refraction surface, the metamaterial surface was cut in steps of three unit cells by one unit-cell, as indicated in Fig. 1(a). The resulting surface stepping was thus on the order of $\lambda/2$.

The surface stepping on the metamaterial sample constitutes a grating, which could be expected to generate a diffracted beam in addition to the zeroth order refracted beam. The condition for the generation of zeroth and higher order beams can be determined from the well known grating formula

$$\sin\theta = \frac{m\lambda}{d} + n\sin\theta_m, \tag{1}$$

where θ_m is the angle of incidence to the normal to the interface from the medium side and θ is the refraction angle. Equation (1) accounts both for refraction (second term) as well as diffraction (first term).

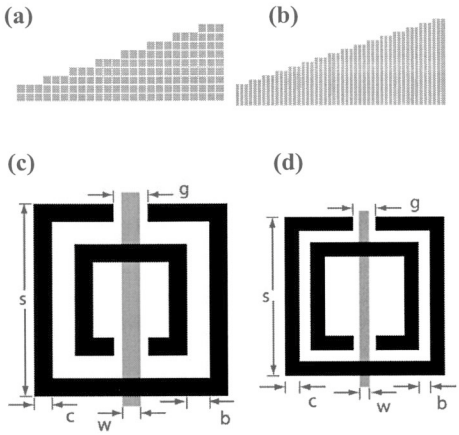

FIG. 1. (a) Schematic diagram of the Shelby *et al.* metamaterial wedge used to demonstrate negative refraction. White lines in the diagram indicate planes on which SRRs and wires are patterned. In this case, the lines indicate SRRs and wires were patterned in two dimensions. (b) Schematic diagram of the 2.5 mm structure. This new structure has a cubic unit-cell 2.5 mm in size, and is patterned in only one dimension, as indicated by the lines. (c) Diagram of the SRR (black lines) and wire (in gray) for the Shelby *et al.* sample, with dimensions: $s = 2.63$ mm, $c = 0.25$ mm, $b = 0.3$ mm, $g = 0.46$ mm, $w = 0.25$ mm. (d) Diagram of the SRR (in black) and wire (in gray) for the 2.5 mm sample, with dimensions: $s = 2.2$ mm, $c = 0.2$ mm, $b = 0.15$ mm, $g = 0.3$ mm, $w = 0.14$ mm. The substrate used is 0.25 mm thick FR4 circuit board ($\epsilon = 3.8$), with a copper thickness of roughly 0.017 mm.

For materials with moderate values of refractive index, when $d \ll \lambda$ no diffracted beams are possible. However, when the grating length is on the order of or greater than the free space wavelength, one or more diffracted beams can be generated, provided the index shift and angle of incidence are of large enough magnitude *and* that the surface scattering is strong enough to couple enough energy into the higher order beam.

The elementary arguments leading to Eq. (1) do not allow the relative coupling of the incident beam to the various possible outgoing beams to be determined. Recently, Depine and Lakhtakia have theoretically analyzed the planewave diffraction from a grating between positive and negative-index materials, and have predicted an enhanced coupling to the diffracted orders [7]. This enhanced coupling can be understood by the following argument. A wave incident on a periodically patterned surface will couple to all transmitted and reflected waves whose wavevectors along the interface match that of the incoming wave (k_x) to within a reciprocal lattice vector (i.e., $k_x + m\pi/d$, where m is an integer). This set of modes includes both propagating components—the zeroth order refracted wave and higher diffracted orders—in addition to evanescent components for which $(k_x + m\pi/d) > w/c$. The reflection and transmission coefficients for the evanescent waves generated at the surface between a positive and a negative-index medium have far greater magnitude than those generated at the surface between two media of the same index sign. In a perturbative sense, the grating modulation leads to a coupling between the incident beam and all diffracted beams, mediated by the evanescent components. As these components can have very large magnitude between positive and negative media, the coupling between the incident beam and higher orders is also correspondingly much larger.

To explore the properties of diffracted beams in a negative-index sample, we simulate a wave incident on the interface between a negative-index wedge and free space, as shown in Fig. 2. The simulation is performed using the driven solution in Ansoft's HFSS, a finite-element based electromagnetic mode solver. The simulated geometry is similar to that used in the experiments, except that the wedge is treated as a homogeneous material with negative ε and μ rather than an array of SRRs and wires. A finite-width incident beam is established by driving one end of a 6 cm wide channel, 1 cm in height, lined with an absorber. The absorber guides the wave to the flat surface of the sample wedge. For the case of a wedge sample with a smooth refraction interface, a single refracted beam is always observed at an angle determined by Snell's law (i.e., no diffracted beams), whether the refractive index is positive or negative.

A surface stepping added to a positive index wedge produces a single refracted beam identical to that of the smooth wedge; however, a surface stepping added to the negative-index wedge shown in Fig. 2 results in the appearance of a second beam. The parameters for the geometry in the simulation presented in Fig. 2 correspond to the sample measured in Ref. [2]. From these parameters, Eq. (1) suggests a zeroth order refracted beam at $-58°$ from the surface normal, and a first order diffracted beam at an angle that depends on the apparent grating length.

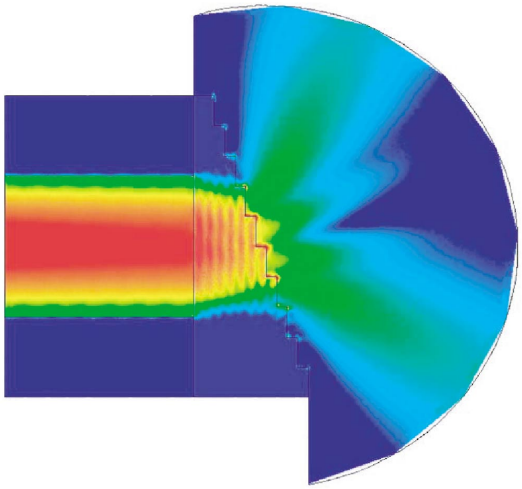

FIG. 2 (color online). Field plot showing the refracted and diffracted beams at the stepped interface of a negative-index wedge. For the wedge in this simulation, $\epsilon = -5.09$ and $\mu = -1.41$, so that $n = -2.68$. The frequency for the simulation is 11.5 GHz. The steps along the refraction surface of the wedge have dimensions 15 mm by 5 mm. In analogy to the experiments, a 1 cm high (in the direction perpendicular to the page) and 6 cm wide guided region is simulated, bounded by electric boundary conditions (parallel to the page). The refracted and diffracted beams exit the slab at angles of $-58°$ and $+30°$, respectively, in agreement with Eq. (1).

Equation (1) indicates that a change in the wavelength of the incident beam with the index of the wedge held constant shifts the angle of deflection of the first order beam, but not that of the zeroth order beam. This can be seen in the angular power spectra presented in Fig. 3. The different curves in Fig. 3 correspond to different values of the incident excitation frequency, which was varied from 9.0 GHz through 11.75 GHz, with all other parameters kept constant. The peak angle of the first order peak as a function of frequency (or wavelength) can be used to empirically determine the value of d, the inverse of which enters as the coefficient to the wavelength in Eq. (1). While the physical surface step size is 15×5 mm, suggesting $d \sim 16$ mm, a fit to the data from Fig. 3 indicates an apparent grating step size of $d = 19$ mm. This extracted value of d fits the observed simulation data well over frequencies from 11.75 GHz down to about 10 GHz.

Below 8.5 GHz, the right hand side of Eq. (1) exceeds unity, and a diffracted beam is no longer possible. We thus

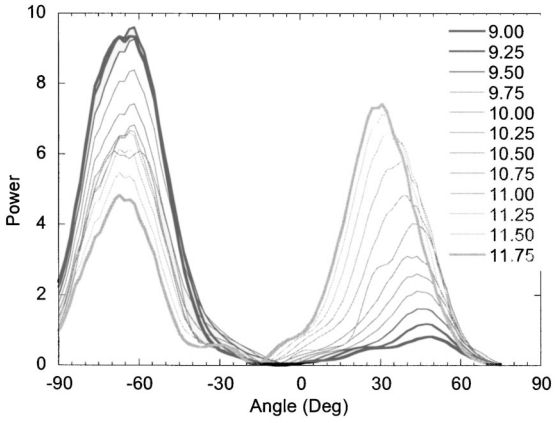

FIG. 3. Simulated angular power spectra at a radius of 10 cm away from the surface of the stepped negative-index wedge of Fig. 3. Each curve corresponds to a different incident wavelength (frequency). All angles are relative to the refraction surface normal.

expect that the coupling strength of the diffracted beam would approach zero near this frequency, which is consistent with the simulation results.

The numerical study of Fig. 3 provides an indication of the relative coupling of the incident wave to the zeroth and first order beams. The relative magnitude of the diffracted peak versus the refracted peak increases as the wavelength becomes smaller, to the point that the diffracted beam can dominate the scattering spectrum. A similar numerical study, in which the frequency was held constant while the surface step size was changed, revealed similar results to those shown in Fig. 3.

While the simulations presented here are based on continuous, homogeneous materials, previous work has indicated that the artificially structured negative-index metamaterials can be well approximated as continuous materials [1–4]. It is thus reasonable to expect that the surface stepping in such metamaterials will lead to the same diffraction phenomenon found in the simulations described above on homogeneous, stepped wedge samples.

The simulations above indicate that for the sample used by Shelby *et al.* [2] a secondary beam should be observed in the frequency regime where the refractive index is negative. A secondary beam was not reported in the initial experiments [2], but was observed in a similar experiment by Houck *et al.*[4]. Because of the design details of the sample, the plates were separated by roughly 2 mm more than the 10 mm (0.4 inch) standard X-band spacing, leading to a source of variability in the experiments.

To further study and clarify experimentally the issue of higher order beams, we perform an angle-resolved mapping of the fields transmitted by each of two different metamaterial wedge samples as a function of frequency. One of the samples is that used by Shelby *et al.*, having the dimensions indicated in Fig. 1(c). The other wedge sample utilized a new unit-cell design shown in Fig. 1(d).

The apparatus used for the experiments is based on a parallel plate waveguide, and is similar in spirit to that used in previous experiments [8]. An incident beam having minimal transverse phase variation is generated by coupling microwaves from an X-band coax-to-waveguide adapter (HP X281A) into a channel of parallel plate waveguide. Absorber (Microsorb Technologies Inc. MTL-73) is patterned so as to gradually widen along the path of the beam from the 0.9 inches width of the adapter, forming an exit aperture of roughly 15 cm (6 inches). The channel is connected to a parallel plate semicircular central chamber, in the center of which is placed the metamaterial sample. The length of the channel (coax adapter to exit aperture) is 40 cm. A waveguide detector is positioned at the radius of the semicircular plates, a distance of 40 cm from the sample, and is capable of being swept over an angular range of nearly 180°.

As a control, the angular distribution of power refracted from a Teflon sample, with the same dimensions and surface step size as the Shelby *et al.* sample, is measured. The result, shown in Fig. 4(a), reveals that the beam was refracted to a positive angle, as expected. No other diffracted beam is detected, although over the frequency range shown, Eq. (1) predicts that a first order mode could occur ($-63°$ at 11.5 GHz, for example).

In contrast to positive index media, negative-index media are inherently frequency dispersive. The expected frequency region of negative refraction for the sample used by Shelby *et al.* was from 10.5 GHz to 11.1 GHz, but these limits are somewhat nebulous due to the positioning of the upper and lower plates relative to the sample. In the present study, the chamber plates are fixed at a distance of 1.27 cm (0.5 inches). As can be seen from Fig. 4(b), at frequencies coincident with the expected negative-index frequency band, the incident beam is indeed bent to negative angles. In addition, as Eq. (1) suggests, there is also a secondary beam at positive angles corresponding to the first order diffracted beam. The position and dispersion of the diffracted beam is consistent with Eq. (1), assuming the value of d derived from the simulation analysis in Fig. 3. The agreement is quite good considering the simplicity of the theory, which assumes a continuous medium. These results suggest that not only does the bulk metamaterial behave as a continuous material with negative refractive index, but also the surface stepping contributes to the properties and can be modeled as steps in an otherwise continuous material.

Both Eq. (1) and the simulations suggest that by reducing the size of the unit cell by a modest amount, effectively reducing the refraction surface grating length, the diffracted beam can be eliminated. Because focusing and other applications rely on the suppression of diffracted

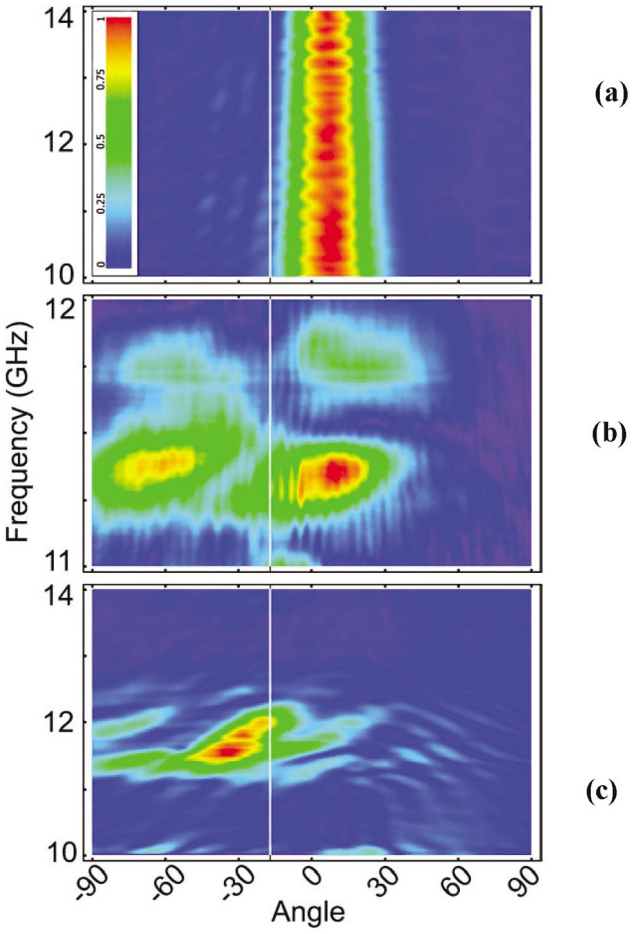

FIG. 4 (color). Map of the transmitted power as a function of frequency (vertical axis) and angle away from direct incidence (horizontal axis), for (a) a Teflon wedge with 15 mm × 5 mm steps; (b) the Shelby *et al.* wedge; (c) the 2.5 mm unit-cell wedge. The vertical white lines indicate the angle of the surface normal.

beams, it is of interest to demonstrate experimentally that an appropriate reduction of the unit-cell size will result in a single negatively refracted beam. To show this, we designed a new metamaterial sample with a cubic unit-cell size of 2.5 mm—half the size of the Shelby *et al.* unit cell in the plane of propagation. The wedge sample is indicated schematically in Fig. 1(b), while the detailed dimensions of the metamaterial unit cell are shown in Fig. 1(d). The refraction surface angle is again 18.4°, and is stepped three unit cells by one unit cell.

A map of the transmitted power as a function of frequency and angle for the 2.5 mm sample is shown in Fig. 4(c). The predicted left-handed band, as determined from simulations on the new unit cell, occurs from 11.3 GHz to 12.2 GHz. The measured spectrum, as anticipated, exhibits negatively refracted power over this band of frequencies, and most importantly no diffracted band appears.

The simulations presented above, as well as the experimental data in Fig. 4, serve to illustrate the role of surface inhomogeneity in refraction experiments on negative-index media. Although the metamaterial samples represent somewhat complicated systems, our results and analysis show that Eq. (1) correctly accounts for the presence of both the zeroth and higher order beams. Furthermore, the results confirm the enhanced coupling to diffractive orders for negative-index samples, as recently predicted by Depine and Lakhtakia [7]. This increased coupling represents an important distinction between the behavior of positive and negative-index media, and suggests that surface periodicity plays a much more significant role in the latter.

The enhanced coupling may be useful for lens applications, where negative-index components have inherent advantages. Recent work has shown, for example, that lenses made of negative-index materials are less aberrant than their positive index counterparts [9]. The dispersion associated with the diffracted order in a stepped negative-index optic may be useful for composite negative-index optical components, in which the advantages of negative-index are combined with other advantageous properties related to diffractive effects. Hybrid lenses, in which a diffractive optic is used to compensate for the chromatic aberration of a lens, are an example where the combination of refraction and diffraction can prove useful [10].

This work was supported by a Multidisciplinary University Research Initiative, sponsored by DARPA/ONR (Grant No. N00014-01-1-0803), as well as DARPA/ARO (Grant No. DAAD19-00-1-0525).

[1] D. R. Smith, W. Padilla, D. C. Vier, S. C. Nemat-Nasser, and S. Schultz, Phys. Rev. Lett. **84**, 4184 (2000).
[2] R. A. Shelby, D. R. Smith, and S. Schultz, Science **292**, 79 (2001).
[3] C. G. Parazzoli, R. B. Greegor, K. Li, B. E. C. Koltenbah, M. Tanielian, Phys. Rev. Lett. **90**, 107401 (2003).
[4] A. A. Houck, J. B. Brock, and I. L. Chuang, Phys. Rev. Lett. **90**, 137401 (2003)
[5] V. G. Veselago, Sov. Phys. Usp. **10**, 509 (1968).
[6] J. B. Pendry, Phys. Rev. Lett., **85**, 3966 (2000).
[7] R. A. Depine and A. Lakhtakia, Phys. Rev. E **69**, 057602 (2004).
[8] A. F. Starr, P. M. Rye, J.J. Mock, D. R. Smith, Rev. Sci. Instrum. **75**, 2244 (2004).
[9] D. Schurig and D. R. Smith, Negative index lens aberrations, lanl.arxiv.org, physics/0403147.
[10] K. J. Weible, A. Schilling, H. P. Herzig, and D. Lobb SPIE Int. Soc. Opt. Eng. **3749**, 278 (1999).